Progr Colloid Polym Sci (2006) 133: 78–87
DOI 10.1007/2882_067

Published online: 6 May 2006

Federica Lo Verso
Christos N. Likos
Luciano Reatto

Star Polymers with Tunable Attractions: Cluster Formation, Phase Separation, Reentrant Crystallization

Federica Lo Verso (✉) · Christos N. Likos
Institut für Theoretische Physik II,
Heinrich-Heine-Universität Düsseldorf,
Universitätsstraße 1, 40255 Düsseldorf,
Germany
e-mail: federica@thphy.uni-duesseldorf.de

Luciano Reatto
Dipartimento di Fisica,
Università degli Studi di Milano,
Via Celoria 16, 20133 Milano, Italy

Abstract We consider a model to describe starlike polymers featuring a steric repulsion accompanied by a dispersion- or depletion-induced tunable attraction. The range and depth of the latter can be controlled by suitable choices of the solvent, salt concentration and/or depletant size and type, whereas the strength of the steric repulsions is set by the arm number f of the stars. We focused on star polymers with arm number $f = 32$. Depending on the choice of the attraction characteristics and on the temperature, the system exhibits, in addition to the usual ultra-soft repulsion, a relatively short range attraction and a secondary repulsive barrier at longer distances. Our results show a variety of structurally distinct states. In the fluid phase we find evidence for cluster formation which is accompanied by fluid-phase separation. Moreover the system presents unexpected fluid-solid transitions which are *completely absent* for the purely repulsive case. The dependence of the cluster and solid regions, and the location of the critical point on the potential parameters is quantitatively analyzed.

Keywords Polymers · Soft colloids · Clusters

Introduction

Soft matter systems are characterized by a high degree of structural complexity. This complexity expresses itself both in terms of the architecture of the constituent particles and in terms of the vast separation of length- and time-scales between the dissolved, mesoscopic aggregates and the microscopic solvent. A statistical mechanical approach towards analyzing such systems would be therefore unfeasible if one attempted to keep track of all degrees of freedom involved. It turns out that an efficient strategy to overcome these difficulties is to integrate out the fast, microscopic degrees of freedom, so that only the mesoscopic ones remain in the picture. The result of this process is the introduction of an *effective interaction potential* between the heavy particles, which is to a large extent induced by the degrees of freedom that have been integrated out [1]. Consequently, the effective interaction potential can be tuned in a number of ways, giving rise to an unprecedented flexibility in controlling the interparticle interactions, a feature absent in atomic systems.

A prominent example of a tunable and, from an atomistic point of view, unusual effective interaction is the one acting between the centers of two star-polymers in good solvents. These macromolecules consist of f chains anchored on a common center [2]. The effective interaction between star polymers shows a logarithmic dependence on their center-to-center separation r for small distances and it crosses over to a Yukawa form for larger ones [3, 4]. Moreover, the overall strength of the interaction scales with temperature and is also proportional to $f^{3/2}$. Thus, f controls the softness of the stars which, formally, reduce to hard spheres in the limit $f \to \infty$.

Due to recent advances in the synthesis of regular, monodisperse stars [5], and to their several medical and industrial applications [2], star-polymer solutions received a great deal of attention in the recent past. In addition, star polymers are excellent model systems as colloids

with tunable softness. Accordingly, there has been a large amount of theoretical [3, 4, 6–15] and experimental [4, 16–26] work pertaining to their equilibrium and rheological properties. Moreover, the non-equilibrium phase behavior of mixtures between stars and linear chains has also attracted considerable attention [27–29]. Here we summarize those findings that are most relevant to the present work. First simulation and theory have shown that a critical functionality $f_c = 34$ exists, below which star polymer solutions never crystallize, at any concentration [10]. Secondly, the density-functionality phase diagram of the stars features several regions of reentrant melting upon density increases [10]. Thirdly, the ideal glass transition lines from Mode Coupling Theory roughly follow the equilibrium crystallization transition [12]. And, finally, experiments and theory have shown that ergodicity can be restored in a dynamically arrested star solution by addition of smaller linear homopolymer [27].

One-component solutions of regular star polymers with a pointlike center, dispersed in an athermal solvent feature the above-mentioned, purely repulsive and entropic effective interaction. However, attractions that must be superimposed to the steric chain repulsion can be present due to a number of additional factors. First, suppose that the polymer chains are grafted on a colloidal particle of finite size b (still $b \ll \sigma$, with σ denoting the chains' spatial extent). In that case, the attraction is caused by the ubiquitous dispersion force between the compact spherical colloids [30, 31]. In fact, grafting of the chains has been originally put forward as precisely a means of providing a steric barrier to counteract this attraction [3]. Further, effective, depletion-like attractions between stars emerge in multicomponent star-chain [28, 29] or star-star mixtures [32], which have been looked upon recently, both in theory and in experiment. Other interesting systems, in this context, are star polymers with attractive polar end groups, telechelic associating polymers with hydrophobic terminal groups and associating polyelectrolytes in homogeneous solutions [33–35]. Theoretical approaches have been developed to describe flower-like micelles with hydrophobic terminal groups that self-assemble in water. Such aggregates show a characteristic "bridging attraction" [36, 37]. Hence, the study of a system interacting by a combination of a starlike repulsion and an additional attraction is physically motivated.

Along these lines, a model potential to describe star-polymer solutions in which, in addition to the excluded volume effects, attractions emerge, has been recently studied [38]. For this model the fluid-fluid phase diagram has been determined using mean field theory and two fluid-state-theories, the modified hypernetted chain closure (MHNC) [39] and the hierarchical reference theory (HRT) [40, 41] for different f-values. If the strength of the interaction is strong enough a fluid-fluid phase transition appears but the density-temperature coexistence curve bifurcates at a triple point into two lines of coexistence terminating at two critical points. This peculiar phase behavior is related to the unusual form of the repulsive contribution. For the same pair interaction, dynamical properties as well as the appearance of glass transition have been studied [13]. The interplay between attractive interactions of different range and ultra-soft core repulsion has been investigated analyzing the effect on the dynamics and on the occurrence of the ideal glass transition line, together with the interplay between equilibrium and non equilibrium phase behavior.

In [13, 38], the parameters were chosen in such a way that the total potential featured just the ultrasoft repulsion at short distances and a pure attraction for longer ones. However, this is not the case, e.g., for depletion-induced attractions: the total potential features both an attractive part and a secondary, repulsive barrier at longer distances. It is the purpose of this paper to analyze quantitatively the behavior of such systems. Our results show a remarkable variety of structural and thermodynamic phenomena, including the formation of clusters, fluid-fluid phase coexistence as well as the emergence of stable solids, which are unstable in the absence of attractions. This paper is organized as follows: in Sect. 2 we introduce the system and the effective interaction we employed. In Sect. 3 we describe the theoretical and numerical tools to study structural properties and phase behavior, whereas in Sect. 4 we present and critically discuss our results. Finally, in Sect. 5 we summarize and draw our conclusions.

The Model System: Effective Pair Interaction

The steric part of effective pair interaction between star polymers with f arms in a good solvent, $v_{st}(r)$, is given by the functional form [4]:

$$\beta v_{st}(r) = \frac{5}{18} f^{3/2} \begin{cases} \left[-\ln\left(\frac{r}{\sigma}\right) + \frac{1}{1+\sqrt{f}/2} \right] & \text{if} \quad r \le \sigma; \\ \frac{1}{1+\sqrt{f}/2} \left(\frac{\sigma}{r}\right) \exp\left[-\frac{\sqrt{f}(r-\sigma)}{2\sigma} \right] & \text{if} \quad r \ge \sigma, \end{cases} \tag{1}$$

where $\beta = (k_B T)^{-1}$, with Boltzmann's constant k_B and the absolute temperature T, and σ is the corona diameter of the stars, related to the experimentally measurable radius of gyration R_g via $\sigma \simeq 1.26 R_g$ [8]. On top of this repulsion, now superimpose an attraction $w(r)$, introducing thereby the total interaction potential $V_{tot}(r) = v_{st}(r) + w(r)$. The form of $w(r)$ follows from the physical motivation put forward in [38]. In order to maintain the $\sim 1/r$-scaling of the effective force $F(r) = -\nabla V_{tot}(r)$ at short distances, the attractive contribution $w(r)$ is chosen to have the form of a Fermi potential, which is essentially constant for small r-values, and whose point of inflection and sharpness are

free parameters. In particular, $w(r)$ reads as:

$$w(r) = -C\left\{\exp\left[\frac{r-A}{B}\right]+1\right\}^{-1}. \quad (2)$$

Let us briefly discuss the meaning of the various parameters and the physical mechanisms that allow them to be externally controlled. C is an energy scale, whereas A and B are length scales. The relevant physical quantity is the reduced temperature

$$T^* \equiv \frac{k_B T}{C}. \quad (3)$$

If the attraction results from dispersion forces, then C can be tuned by modifying the solvent that affects the value of the Hamaker constant [30, 31]. In this case, C is temperature-independent and the system is thermal. If the attraction is caused due to the addition of athermal depletants (such as polymer coils [28, 29] or smaller stars [32]), then C scales with $k_B T$, hence temperature is irrelevant, but it acquires a dependence on the depletant concentration. In this case, the above-defined quantity T^* can be interpreted, roughly, as an inverse depletant reservoir concentration. The length scales A and B can also be tuned externally. In the case of dispersion-induced attraction, they can be influenced by screening the dipole–dipole interaction through addition of salt, which remains mainly in the intermolecular space, not affecting therefore the conformation of the stars. In the case of depletant-induced attraction they can be influenced by modifying the softness and size of the smaller component.

For this model, the case in which the full potential, $V_{tot}(r)$, is deprived of secondary maxima at large $r \gtrsim \sigma$ has been previously discussed in detail, focusing on the equilibrium phase diagram [38] and the presence of glass transitions [13]. Some peculiar and interesting characteristics have been found, such as, e.g., the existence of *two* critical points and, for $46 \lesssim f \lesssim 70$ and shrinking the well potential, a progressively shift of the glass region to higher density. Moreover, it has been shown that for a two-component asymmetric star-star mixture, the introduction of small depletant stars determine, for certain ranges of f and density of the depletant, an attractive contribution to the interaction plus a repulsive bump for long distances [32]. In that case, the big-macromolecules in solution have a high arm number, $f \simeq 270$ value. The phase diagram of asymmetric mixture has been considered, finding in particular that the addition of small stars melts the crystal formed by the big ones.

In this paper we modify the parameters A and B in order to analyze the effect of the repulsive barrier on the interaction that we obtain by "shrinking" the well potential, moving at the same time the minimum to lower interparticle separations. In order to avoid excessive freedom associated with many parameters, we fix the value of A to $A = 1.35\sigma$ throughout and the functionality to $f = 32$, varying solely the parameter B that controls the sharpness of the Fermi potential, (Eq. 2). In Fig. 1a we show the total interaction potential $V_{tot}(r)$ for the three values of B employed in this work, $B = 0.15\sigma$, 0.1σ, and 0.05σ. It can be seen that decreasing B has the effect of lowering the depth of the attractive well, reducing its range and enhancing the height of the secondary, repulsive barrier. In the same Figure, we also show the potential shape for the choice of parameters employed in previous work [38], namely $A = 2.1\sigma$ and $B = 0.35\sigma$. Here, it can be seen that $V_{tot}(r)$ is free of repulsive barriers and that the attraction is much deeper and longer in range. In Fig. 1b we see that for high enough temperatures, $T^* \gtrsim 2.0$, $V_{tot}(r)$ essentially reduces to the purely repulsive interaction $v_{st}(r)$, as the thermal energy is sufficiently strong to wash out the attraction. Finally, in Fig. 1c we show the Fermi-like attraction $w(r)$ for the same combination of A- and B-values as in Fig. 1a.

The reasons to focus on star polymers with functionality $f = 32$ are many fold. First, we wish to analyze here a typical intermediate-functionality case right between the polymer-like ($f \gtrsim 1$) and the colloid-like ($f \gg 1$)-limits. Secondly, $f = 32$ is a truly interesting case: below this value the purely repulsive star solution as well as the model attraction considered till now (i.e., without repulsive bump and with a long range attraction [38]) is always fluid changing the relevant thermodynamic parameters. Thus, for this *borderline* case the peculiar features with respect to the previously analyzed cases are more evident. And, finally, $f = 32$-arms star polymers are quite common experimentally, since they can be synthesized by growing

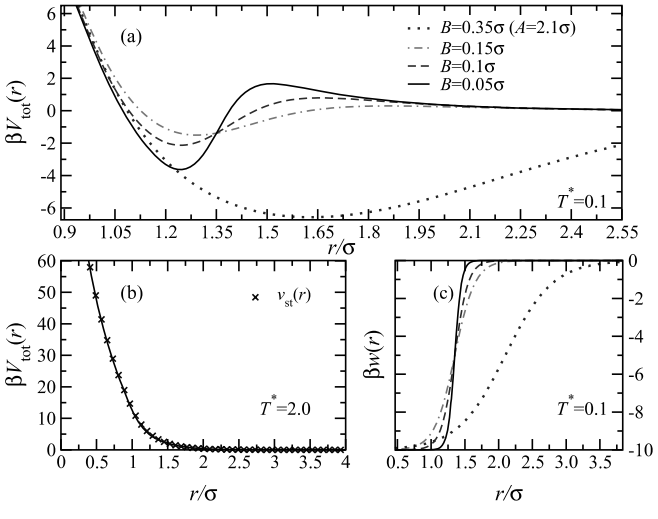

Fig. 1 **a** The total interaction potential $\beta V_{tot}(r)$, versus the interparticle separation $r^* = r/\sigma$ for temperature $T^* = 0.1$, $f = 32$ and several value of the parameter B in Eq. 2. The *dotted line* shows a case considered in [38]. **b** Comparison between $T^* = 2.0$ for $B = 0.05\sigma$ and the purely repulsive interaction. **c** The attractive contribution $w(r)$ for the B-values of panel (**a**)

living polymers on the reaction sites located at the ends of dendritic cores.

Modified Hypernetted Chain (MHNC) Integral Equation

Our analysis is based on the examination of the pair correlation functions of the system, in particular the radial distribution function $g(r)$ and the structure factor $S(q)$ [42]. The latter depends on the momentum transfer $\hbar q$ in a scattering experiment, q being the magnitude of the scattering wavevector. The relation between $S(q)$ and $g(r)$ reads as:

$$S(q) = 1 + \rho \int \mathrm{d}^3 r e^{-\mathrm{i}\boldsymbol{q}\cdot\boldsymbol{r}} [g(r) - 1] \,, \tag{4}$$

where ρ is the density of the system. We define the dimensionless density ρ^* as

$$\rho^* = \rho\sigma^3 \,. \tag{5}$$

The pair correlation functions can be calculated for any given interaction potential and thermodynamic parameters (ρ^*, T^*) by employing approximate closures to the Ornstein–Zernike relation [42], resulting thereby in a variety of integral equation theories for uniform fluids. In this work, we employ the modified hypernetted chain (MHNC) integral equation [39], which is very accurate, both for purely repulsive potential as well as in presence of attractive contribution. In the particular case of star polymers, the high accuracy of this theory to describe fluid and metastable states in good solvent [12] as well as in presence of attractive contributions [13, 38] has been verified for a large range of f, density values and temperatures.

From a cluster expansion origin, one obtains the exact relation connecting the radial distribution function $g(r)$ to any given interparticle potential $\phi(r)$:

$$g(r) = \exp[-\beta\phi(r) + g(r) - 1 - c(r) + E(r)] \,, \tag{6}$$

where $E(r)$ is the bridge function and $c(r)$ the direct correlation function [42], related to $g(r)$ with the aforementioned Ornstein-Zernike relation:

$$g(r) - 1 = c(r) + \rho \int \mathrm{d}^3 r' [g(|\boldsymbol{r}' - \boldsymbol{r}|) - 1] c(r') \,. \tag{7}$$

In the MHNC scheme, the exact bridge function $E(r)$ is replaced by that of a fluid of hard spheres, $E_{\mathrm{HS}}(r)$, of a suitably chosen diameter d. To optimize this choice, which depends on the parameter d, the free energy is minimized [39] via the relation:

$$\int \mathrm{d}\boldsymbol{r} \, [g(r) - g_{\mathrm{HS}}(r; \eta_{\mathrm{HS}})] \, \frac{\partial E_{\mathrm{HS}}(r; \eta_{\mathrm{HS}})}{\partial \eta_{\mathrm{HS}}} = 0 \,, \tag{8}$$

where $\eta_{\mathrm{HS}} = \pi\rho d^3/6$ is the packing fraction of the effective hard sphere system and $g_{\mathrm{HS}}(r, \eta_{\mathrm{HS}})$ the radial distribution function of the same. Verlet and Weis [43] provided an accurate parametrization of $g_{\mathrm{HS}}(r, \eta_{\mathrm{HS}})$ based on the Percus–Yevick solution, with a correction which incorporates thermodynamical consistency through the Carnahan-Starling state equation [42]. This, together with Eqs. 6–8 gives a closed set of equations which are solved by a standard iterative method. The dependence of η_{HS} on the density as determined by Eq. 8 reflects the peculiar features of the interparticle interaction [38].

Results and Discussion

We analyzed three different solutions of star polymers in presence of attractive interactions, modeled by Eq. 2, all with functionality $f = 32$ and at fixed $A = 1.35\sigma$. As mentioned before, three different values of the parameter B were examined, namely $B = 0.15\sigma$ (system code SP-B.15), $B = 0.1\sigma$ (system code SP-B.1), and $B = 0.05\sigma$ (system code SP-B.05). At fixed temperature, a decrease in B has the effect of increasing the depth of the attractive well, shrinking its range and at the same time increasing the height of the accompanying repulsive bump. Our goal is to gain insight into the influence that these changes of the interparticle potential have on the phase diagram of the system and to quantify the effects of the competition between a relatively short-range attraction and a longer-range repulsion in a system with a peculiar ultra-soft repulsive core. Though systems with a combination of attraction and a repulsive hump have been studied in the past [44–50] the short-range steric repulsion has always been steep; the presence of the ultrasoft repulsion in our system, which is not able to support stable crystals in and of its own [10, 38] provides an additional novel aspect of the system at hand.

Unlike purely repulsive star polymers, in the present system the temperature is a relevant thermodynamic variable. We begin with a relatively high temperature, $T^* = 2.0$. In Fig. 2 we show the structure factor of the SP-

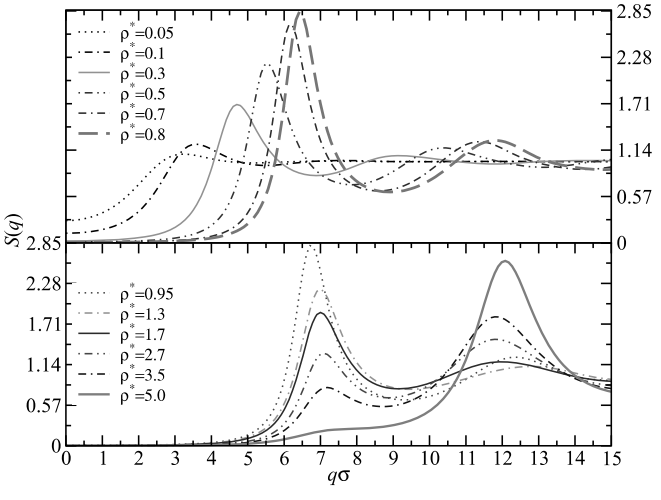

Fig. 2 Structure factor of the SP-B.15-model for at $T^* = 2.0$

B.0.15 system at this temperature and for a wide range of densities. We found essentially the same structure factors obtained for purely repulsive one component stars [6]. Indeed, at sufficiently high temperatures, the Fermi contribution to our model-interaction becomes unimportant because it is washed out by the thermal energy. Thus, the anomalous dependence of $S(q)$ on density, known from usual star polymers, is recovered. Starting at low densities, the first peak of $S(q)$ grows in height and moves to higher q-values, which scale as $\sim \rho^{1/3}$, up to the overlap density $\rho^* \simeq 0.8$. For higher values of the density, the main peak height starts decreasing, the second peak height starts increasing (eventually replacing the first peak as the highest) and the peak positions become density-independent. All these features arise from the interplay between the long-distance Yukawa decay of the interaction of Eq. 1 and its short-distance ultrasoft, logarithmic dependence. Below the overlap density, the former is felt, giving rise to normal structure factors, whereas above the overlap density the logarithmic repulsion causes the peak anomalies. These features have been analyzed in detail in [6]. For the whole density range, the peaks in the structure factor never exceed the value of 2.85: in agreement with the Hansen–Verlet criterion [51], this means that the system is always a fluid, an assertion explicitly confirmed by extensive Monte-Carlo simulations [10] and in full agreement with experimental results [21]. The indistinguishability of the structure factors at $T^* \gtrsim 2.0$ from those of the purely repulsive system has been found for all three systems studied, SP-B.0.15, SP-B.0.1, and SP-B.0.05.

Let us now look at the effects of decreasing the temperature. We examined temperatures in the range $0.1 \leq T^* \leq 2.0$, whereas the density was varied in a wide range, typically $0 \leq \rho^* \leq 10.0$. In Fig. 3 we present the structure factor for the system SP-B.15 at $T^* = 0.1$, which shows marked differences as compared with the same quantity at $T^* = 2.0$, Fig. 2. For small densities $\rho^* = 0.04$, (Fig. 3, upper panel), we can already observe a value of $S(q = 0) > 1$, which is a signature of a neighboring spinodal, on which $S(q = 0)$ diverges. At the same time, more unusual features of $S(q)$ show up. Unlike its high-temperature counterpart, $S(q)$ has two distinct peaks, a pre-peak at $q\sigma \simeq 1$, whose position moves to higher q-values with increasing density and a main peak at $q\sigma \simeq 6$, whose position is strictly *density-independent*, up to a density $\rho^* \lesssim 0.6$. These characteristics carry the signature of *cluster formation* within the uniform fluid [47]. The interparticle potential features a minimum at $r_{\min} \simeq 1.3\sigma$, which leads to particle aggregation with an interparticle separation $r_{\min}$. The accompanying repulsive barrier limits the growth of the aggregates, leading thereby to the formation of finite clusters of a typical size $R_{\rm cl}$ and intercluster separation L. As the length scale $r_{\min}$ is set by the interaction and not by the concentration, the particle–particle distance within a cluster manifests itself, in momentum space, in the form of a density-independent peak at $q \simeq 2\pi/r_{\min}$. The low-q pre-peak, on the other hand, is the cluster-peak that is related to the intercluster separation as $q \simeq 2\pi/L$. Indeed, as the density grows, the clusters approach each other, resulting into the observed displacement of the cluster peak to higher q-values. At a density $\rho^* \simeq 0.6$ the cluster peak disappears altogether. We interpret this as a merging of different clusters, which leads to the loss of cluster identity and thus leaves individual particles as the only distinguishable scattering units in the system. This assertion is corroborated by the fact that for $\rho^* \gtrsim 0.6$ the particle–particle peak, which was previously density-independent in its location, now does shift to higher q-values with increasing ρ.

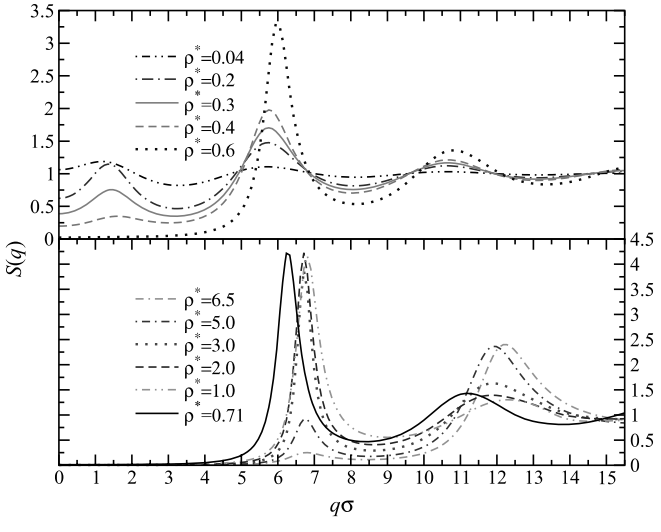

Fig. 3 Structure factor for the system SP-B.15 at $T^* = 0.1$. *Top*: notice the appearance of a low-density small peak. *Bottom*: for high density the main peak of the structure factor is considerably higher than 2.85 at $\rho^* = 1.0$

In Fig. 3, lower panel, we see how $S(q)$ then further develops upon density increase. Whereas the main peak position shifts to higher q's up to a density $\rho^* \simeq 1.0$, the usual star-polymer scenario [6] takes over thereafter: the position of the main peak does not evolve with ρ^*, its height decreases and that of the second peak increases, as in the purely repulsive case. These effects are due to the ultrasoft logarithmic divergence of the potential. Yet, a very important *quantitative* difference with respect to the case $T^* = 2.0$ shows up: the *height* of the main $S(q)$-peak now markedly exceeds the Hansen–Verlet value 2.85, clearly pointing to the possibility that the added attractions now *stabilize* a crystal that is thermodynamically unstable in their absence.

The same behavior has been found for the systems SP-B.1 and SP-B.05; selected, representative results are shown in Figs. 4 and 5, respectively. Referring to Fig. 4 and in comparison with Fig. 3, we see that the effect of reducing the value of B is to enhance the growth of the height of the principal peak of $S(q)$ at a given temperature.

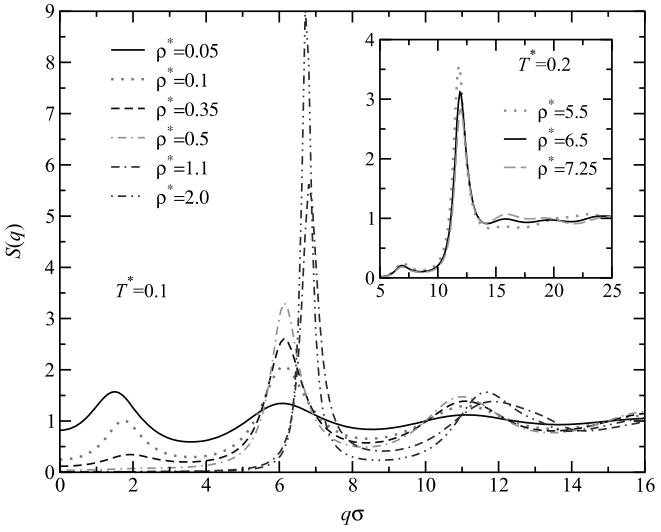

Fig. 4 Structure factor of the SP-.1-system at $T^* = 0.1$. In the *inset*, we show the trend of $S(q)$ for high densities and $T^* = 0.2$ at increasing densities

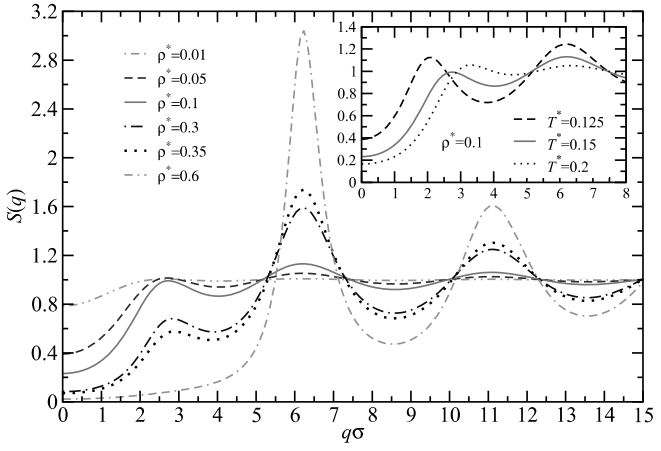

Fig. 5 Structure factor for for the system SP-.05 at $T^* = 0.15$ for several densities. *Inset*: structure factor for fixed density $\rho^* = 0.1$ changing the temperature

Otherwise, clustering is still clearly visible at, roughly, the same range of densities as in the case $B = 0.15$. Once again, we discover that the position of the highest peak does not change with concentration and it is accompanied by a cluster pre-peak, whose position moves to slightly higher q-values. In the inset of Fig. 4, we see the evolution of $S(q)$ for much higher densities: it can be seen that the particle peak at $q\sigma \simeq 7$, which used to be quite high at lower densities, has all but disappeared and the peak at $q\sigma \simeq 12$ has taken its role as the main one [6]. Yet, even this second peak diminishes now in height upon increasing ρ. In conjunction with the Hansen–Verlet freezing rule, this points to a reentrant melting scenario, similar to the one occurring in usual star polymers [10] or in other systems interacting by means of ultrasoft potentials [52, 53].

In Fig. 5, the evolution of the structure factor for the system SP-B.05 is shown. Note that here we had to move to a higher temperature than in the preceding cases, $T^* = 0.15$, because large parts of the $T^* = 0.10$-isotherm are, for this system, subcritical (see below). In the main plot of Fig. 5, the evolution of $S(q)$ with density is shown, featuring once again the typical characteristics of cluster formation. More insight into the nature of the clusters and the incipient macroscopic phase separation can be gained by looking at $S(q)$ at *fixed* density and *lower* temperatures, shown the inset of Fig. 5. Here, it can be seen that the position of the particle–particle peak of $S(q)$ hardly moves upon temperature changes. However, the cluster peak moves to lower q-values, signaling a growth of the cluster size $R_{\rm cl}$ and, concomitantly, the cluster separation L. At fixed density, this corresponds to a growth of the population of the individual clusters, i.e., the number of particles participating in a particular cluster. Consequently, the intercluster separation grows, and the compressibility of the system, which is proportional to $S(q = 0)$ [42], increases as well. Further lowering of the temperature leads then to a formation of a cluster of macroscopic dimensions. The local minimum of $S(q)$ at $q = 0$ turns into a maximum at the Lifshitz line [54, 55] and at the spinodal line this maximum diverges. In other words, a macroscopic phase separation into two fluids at different concentration takes place.

Before proceeding into a quantitative description of all phenomena associated with such systems (clustering, condensation, and crystallization), it is informative to take a look at the emergence of clustered phases in real, as opposed to reciprocal, space. In Fig. 6 we show the radial distribution function $g(r)$ for all three systems considered here at fixed density $\rho^* = 0.05$ and temperature

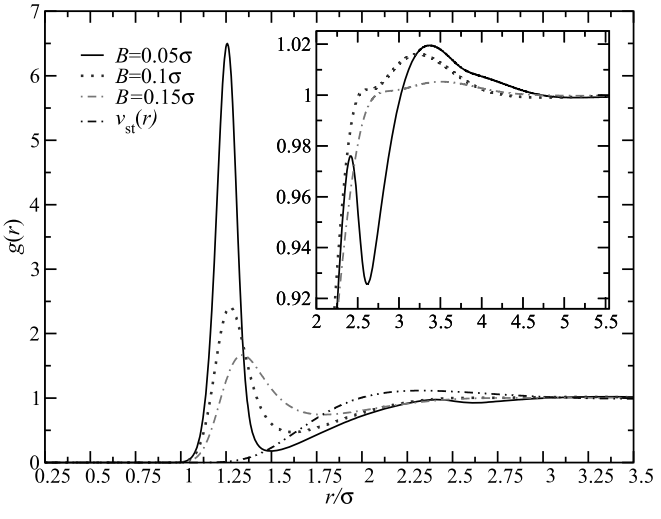

Fig. 6 The radial distribution function $g(r)$ of the systems considered in this work at density $\rho^* = 0.04$ and temperature $T^* = 0.125$. *Inset*: detail of the second peak region

$T^* = 0.125$, together with the same quantity for the purely repulsive star polymer solution interacting by means of the potential of Eq. 1. Whereas the radial distribution function of the latter is rather flat and has a very weak maximum at $a \simeq \rho^{1/3}$, the corresponding quantities for the models SP-B.15, SP-B.1, and SP-B.05 are very different. A pronounced maximum at $r = r_{\min}$ can be seen, clearly signaling the tendency of the particles to stick together at this distance. Note, however, at the same time, the depression at distances $1.5 \lesssim r/\sigma \lesssim 2.0$, arising from the repulsive barrier, which limits the growth of the clusters. Moreover, it can be clearly seen that the stiffness of the clusters is most pronounced for the SP-B.05-system, which features the deepest and shortest-range attraction, together with the strongest repulsive bump. In the inset of Fig. 6, we show the region around the second peak of $g(r)$. For SP-B.15 a broad second peak appears around $r/\sigma = 3.5$, this distance roughly corresponding to the cluster–cluster separation. Decreasing B we can observe a more structured second peak. In particular, for SP-B.05 there is a small additional first peak around $r/\sigma = 2.5$ which can be interpreted as a weak second-shell of neighbors within a given cluster. The height and the number of the peak around $r/\sigma = 3.5$ increases with the density until, as sufficiently high ρ^*, the clusters come close to each other, merge, and thereafter the radial distribution function recovers a shape that describes a usual, unclustered fluid.

The competition between attraction, which favors cluster formation for low T^*, and long range repulsion that favors small aggregates [47,48], is evident under consideration of all three cases investigated. Whereas the occurrence of macrophase separation is sharply defined through the *divergence* of $S(q)$ at $q = 0$, marking the spinodal line of the system, cluster formation in a thermodynamically stable fluid is not associated with any accompanying phase transition. In this respect, the emergence of clusters on a supramolecular scale is akin to the formation of mesoscopic spatial structures in other soft matter systems, such as the random, "sponge" phase in ternary mixtures of oil, water and amphiphilic surfactants [56]. Indeed, also in this case, there is no clear phase boundary between the sponge- and random-mixture states, and one has to resort to somewhat arbitrary structural criteria in order to delineate the regions of stability of the two [54–56]. In our case, we decided to use the existence of the cluster pre-peak in $S(q)$ at low but finite q-values in order to characterize a clustered fluid. In particular, we introduce the criterion than whenever the pre-peak local maximum exceeds the neighboring local minima by more than 0.05, the fluid consists of clustered superstructures.

In Fig. 7 we show the cluster regions as well as the spinodal curves for the systems we investigated. For fixed B, an increase in temperature reduces the range of stability of the cluster region, due to the reduction of the attractive forces in our system. Decreasing B leads to a broadening of the region of the clustered fluid. This behavior is connected to the intensity of the attraction which for such low density has to be strong enough to determine cluster aggregation. In the same figure, the spinodal curves are shown as well: the critical temperature increases with decreasing B and the critical density moves to slightly lower densities. This trend is in agreement with the evolution of the second virial coefficient $B_2(T)$ of the interaction potential, which becomes more and more negative, at fixed temperature, passing from SP-B.15 to SP-B.1 and finally to SP-B.05. More precisely, at $T^* = 0.1$, we have $B_2 = -0.13\sigma^3$ for SP-B.15, $B_2 = -0.20\sigma^3$ for SP-B.1, and $B_2 = -2.66\sigma^3$ for SP-B.05. To provide a comparison, we calculated this coefficient also for the case investigated in [38], which is free of repulsive barriers, finding a value $B_2 = -4.59\sigma^3$ at the same temperature. This is consistent with the result that the critical temperature there has a high value, $T^*_{\text{crit}} = 0.623$ (MHNC calculation).

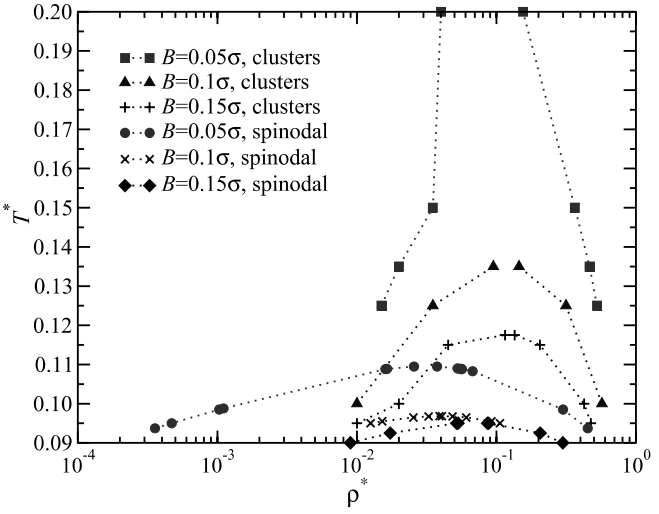

Fig. 7 Cluster region and fluid–fluid coexistence region as delimited by the spinodal line

The occurrence of finite-size clusters in the system is a direct consequence of the existence of a repulsive potential barrier that accompanies the short-range attraction. In this respect, our results are in line with a wealth of theoretical [45–49] and experimental [29,50] results in three-dimensional systems as well as with a recent theoretical analysis of a two-dimensional model that shows the formation of stable circular and stripe patterns [44]. The phenomena observed here can be understood in terms of the competition between the (generally complex) poles of the structure factor $S(q)$ [46,57,58]. Let $q_{\text{R}} + \text{i}q_{\text{I}}$ be such a pole, with q_{R} and q_{I} denoting its real and imaginary parts, respectively. If $q_{\text{i}} = 0$ and $q_{\text{R}} \neq 0$, then the fluid is thermodynamically unstable with respect to *microphase separation*, i.e., ordered microstructures of wavelength $\lambda = 2\pi/q_{\text{R}}$, such as lamellae or periodic crystals, spontaneously form. On the other hand, the case $q_{\text{i}} = 0$ *and* $q_{\text{R}} = 0$ leads to a spinodal curve and *macrophase separa-*

tion. In the case of the systems we examined, the former pole does not occur, but the imaginary part q_i is sufficiently small, so that the cluster pre-peak shows up. At appropriate thermodynamic conditions, the second type of pole occurs and the system phase-separates. The system at hand shows a tendency to form microregions of clustered particles, however true microphase separation is inhibited. The structure factor pre-peak remains finite and the cluster phase possesses full translational symmetry (uniform fluid). Under competition between the attractive plus repulsive parts of the potential, we expect the cluster peak to become the dominant feature of $S(q)$, leading to true microphase separation which at least in $2D$ gives rise to a thermodynamic signature in terms of a peak in the specific heat [44].

Depending on the potential parameters, only one, both, or none of the two scenarios regarding the existence of real poles of $S(q)$ will materialize. In some cases, the existence of the repulsive barrier may lead to a complete disappearance of the spinodal line, which would be otherwise present under the influence of the attraction alone. Here, we rather have a situation in which the repulsive barrier suppresses the critical point without altogether eliminating it, in agreement with the recently studied case of mixtures between multiarm star polymers and depleting, homopolymer chains [29].

Finally, we briefly discuss the occurrence of stable crystals in the system, which are unstable both in the complete absence of attractions [10] and in the presence of long-range, smooth attractions [38]. The very high values of the structure factor peak, see Figs. 3–5, are a clear structural signature of the stability of crystal phases. Moreover, there exist regions in the density-temperature plane, deep in the solid, where the MHNC fails to converge or yields physically unacceptable results, e.g., negative parts of $S(q)$. Thus, the interactions at hand give rise to freezing transitions. Tracing out the precise phase boundaries would require the calculation of the free energies of the competing, fluid and solid phases. This is a cumbersome task, which is additionally complicated by the fact that the precise crystal structure is unknown. Therefore, we resort here to a structural criterion to delineate roughly the freezing lines, namely we trace out the locus of points for which the maximum of $S(q)$ attains the Hansen–Verlet value 2.85. This approach has been shown to reproduce phase boundaries quite well, even for ultrasoft potentials, such as the Gaussian interaction [52]

In Fig. 8 we describe the full "phase diagram", drawn under the procedure described above. The system shows a spinodal line, a cluster line and a line of crystallization. The solid region increases with decreasing B. Irrespective of quantitative details, we can distinguish within the solid region two structures: one region centered around $\rho^* = 0.85$ plus a tail for higher densities. The first region is connected to the evolution of the main peak of $S(q)$, which corresponds to the first peak for $\rho^* \gtrsim 0.6$.

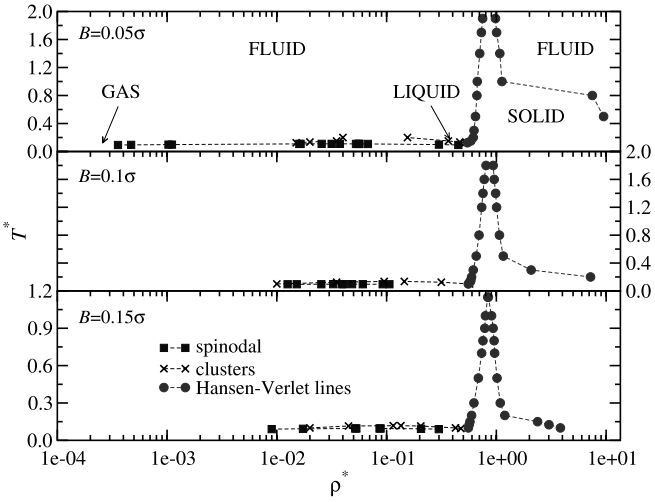

Fig. 8 Full "phase diagrams" for SP-B.15, SP-B.1, and SP-B.05

The second density region is connected to the evolution of the second peak in the structure factor. We observe that for SP-B.15 and $\rho^* \gtrsim 5.0$, the first/main peak disappears and the second peak becomes the main one, but for all the temperatures investigated this peak did not exceed the value 2.85. On the contrary, for SP-B.1 and SP-B.05 there exist some regions where the second peak in the structure factor becomes higher then 2.85 and the first peak becomes lower than this value, at temperatures around $T^* \lesssim 0.4$ and $T^* \lesssim 0.8$, respectively. In this high density tail, we can have small intervals of reentrant melting.

The stabilization of the crystal phase is an effect of the attractive part of the potential and of its range. Indeed solid phases are not present neither for the purely repulsive interaction or for the case studied e.g., in [38] where the attractive interaction is really longer ranged. Changing density and temperature, for the three different model attractions, we could have also a change in the symmetry of the lattice in relation to the position of the repulsive bump with respect to characteristic nearest neighbor and second neighbor distances. The observed trend of broadening of the region of stability of the solid upon shrinking of the attractive well is fully consistent with previous results on the double Yukawa system [59]. Contrary to the case of [59], however, our freezing transition is *forced* to disappear at sufficiently high temperatures, since then we recover the purely repulsive case, which does not support stable solids. Consequently, the freezing line is of *reentrant* type, similarly to the case of the Gaussian model [52] or indeed a whole class of ultrasoft potentials [53].

Finally, we remark that for high densities and low temperatures, $T^* \ll 0.1$ we found evidence of the increasing of $S(q = 0)$, signaling the appearance of a fluid–fluid phase separation, in agreement with the occurrence of a second critical point ($\rho^* = 1.96$, $T^* = 0.247$) in [38]. However,

for such a low temperature and high density, this region is metastable with respect to the freezing.

Conclusions

We have examined the structural and thermodynamic behavior of a system of intermediate-functionality star polymers with additional attractions. The resulting total potential features the original, logarithmic repulsion for close interparticle approaches, dressed with a short-range attraction, which is followed by a repulsive hump at large separations. This is a flexible and tunable system, since the characteristics of the interaction can be tuned by, e.g., suitable choices of smaller polymeric entities to be added to the star polymer solution. We found a wealth of new phenomena, such as a fluid–fluid phase separation, accompanied by a formation of clusters in the stable fluid at supercritical temperatures. The internal structure of the clusters can not be resolved with the tools at hand and it will be the subject of future work. Moreover, the attraction brings about a stabilization of crystal phases, which cannot be supported by the ultrasoft repulsions alone, for the functionality value $f = 32$ studied here. This freezing transition features a maximum crystallization temperature and is reentrant along the density axis.

A number of questions open up, which are related to both the equilibrium and the dynamical behavior of the system at hand. The crystal structures should be identified and the question should be answered as to whether we have polymorphic transitions between lattices of different symmetry. To this end, the powerful tool of genetic algorithms [60] can be employed, to allow for a bias-free search of the crystal structures. Associated with freezing is the possibility of formation of repulsive glasses, in analogy with the case of usual star polymers, for which indeed the region of ideal glass formation is strongly correlated with the domain of stability of the solid [12]. In this respect, the depletants here could have an effect *opposite* to that seen for multiarm star polymers [27]: whereas for $f \gg 1$ added chains *melt* the glass formed by the stars, in our case the exciting possibility opens up that they might *induce* a glass transition in a system that shows no vitrification, at arbitrary densities [12]. At the same time, the property of this system to form clusters makes it possible that a *gelation* transition could find place at *low* densities, in analogy with the recently-studied case of Sciortino et al. [47]. Application of computer simulations and Mode-Coupling Theory should help clarify the questions of the types of arrested states that can occur in our system. The investigation of these questions is the subject of ongoing work.

Acknowledgement This work was funded in part by a grant of the Marie Curie Programme of the European Union, contract number MRTN-CT2003-504712, and in part by the Deutsche Forschungsgemeinschaft (DFG) within the SFB-TR6, Project Section C3.

References

1. Likos CN (2001) Phys Rep 348:267
2. Grest GS, Fetters LJ, Huang JS, Richter D (1996) Adv Chem Phys XCIV:67
3. Witten TA, Pincus PA (1986) Macromolecules 19:2509
4. Likos CN, Löwen H, Watzlawek M, Abbas B, Jucknischke O, Allgaier J, Richter D (1998) Phys Rev Lett 80:4450
5. Zhou L-L, Roovers J (1993) Macromolecules 26:963
6. Watzlawek M, Löwen H, Likos CN (1998) Phys J: Condens Matter 10:8189
7. Likos CN, Löwen H, Poppe A, Willner L, Roovers J, Cubitt B, Richter D (1998) Phys Rev E 58:6299
8. Jusufi A, Watzlawek M, Löwen H (1999) Macromolecules 32:4470
9. Witten TA, Pincus PA, Cates ME (1986) Europhys Lett 2:137
10. Watzlawek M, Likos CN, Löwen H (1999) Phys Rev Lett 82:5289
11. Dzubiella J, Likos CN, Löwen H (2002) Chem J Phys 116:9518
12. Foffi G, Sciortino F, Tartaglia P, Zaccarelli E, Lo Verso F, Reatto L, Dawson KA, Likos CN (2003) Phys Rev Lett 90:238301
13. Lo Verso F, Reatto L, Foffi G, Tartaglia P, Dawson KA (2004) Phys Rev E 70:061409
14. Benzouine F, Benhamou M, Himmi M (2004) Eur Phys J E 13:345
15. Benhamou M, Himmi M, Benzouine F, Bettachy A, Derouiche A (2004) Eur Phys J E 13:353
16. Dozier WD, Huang JS, Fetters LJ (1991) Macromolecules 24:2810
17. Richter D, Jucknischke O, Willner L, Fetters LJ, Lin M, Huang JS, Allgaier J, Roovers J, Toporowski C, Zhou L-L (1993) Physique J IV 3:3
18. Willner L, Jucknischke O, Richter D, Roovers J, Zhou L-L, Toporowski PM, Fetters LJ, Huang JS, Lin M, Hadjichristidis N (1994) Macromolecules 27:3821
19. Kapnistos M, Vlassopoulos D, Fytas G, Mortensen K, Fleischer G, Roovers J (2000) Phys Rev Lett 85:4072
20. Loppinet B, Stiakakis E, Vlassopoulos D, Fytas G, Roovers J (2001) Macromolecules 34:8216
21. Vlassopoulos D, Fytas G, Pakula T, Roovers J (2001) Phys J: Condens Matter 13:R855
22. Bang J, Lodge TP, Wang X, Brinker KL, Burghardt WR (2002) Phys Rev Lett 89:215505
23. Lodge TP, Bang J, Park MJ, Char K (2004) Phys Rev Lett 92:145501
24. Bang J, Lodge TP (2004) Phys Rev Lett 93:245701
25. Stellbrink J, Rother G, Laurati M, Lund R, Willner L, Richter D (2004) Phys J: Condens Matter 16:S3821
26. Laurati M, Stellbrink J, Lund R, Willner L, Richter D, Zaccarelli E (2005) Phys Rev Lett 94:195504
27. Stiakakis E, Vlassopoulos D, Likos CN, Roovers J, Meier G (2002) Phys Rev Lett 89:208302

28. Stiakakis E, Petekidis G, Vlassopoulos D, Likos CN, Iatrou H, Hadjichristidis N, Roovers J (2005) Europhys Lett 72:664
29. Likos CN, Mayer C, Stiakakis E, Petekidis G (2005) Phys J: Condens Matter 17:S3363
30. Russel WB, Saville DA, Schowalter WR (1989) Colloidal Dispersions. Cambridge University Press, Cambridge
31. Pusey PN (1991) In: Hansen J-P, Levesque D, Zinn-Justin J (eds) Les Houches, Session LI, Liquids, Freezing and Glass Transition. North-Holland, Amsterdam
32. Mayer C, Likos CN, Löwen H (2004) Phys Rev E 70:041402
33. Pitsikalis M, Mays JW, Hadjichristidis N (1996) Macromolecules 29:179
34. Vlassopulos D, Pakula T, Fytas G, Pitsikalis M, Hadjichristidis N (1999) Chem J Phys 111:1760
35. Clément F, Johner A, Joanny J-F, Semenov AN (2000) Macromolecules 33:6148
36. Semenov AN, Joanny J-F, Khokhlov AR (1995) Macromolecules 28:1066
37. Bhatia SR, Russel WB (2000) Macromolecules 33:5713
38. Lo Verso F, Tau M, Reatto L (2003) Phys J: Condens Matter 15:1505
39. Lado F, Foiles SM, Ashcroft NW (1983) Phys Rev A 28:2374
40. Parola A, Reatto L (1984) Phys Rev Lett 53:2417; Phys Rev A 31:3309 (1985)
41. For an ample review of the HRT, see: Parola A, Reatto L (1995) Adv Phys 44:211
42. Hansen JP, McDonald IR (1986) Theory of Simple Liquids, 2nd edition. Academic, London
43. Verlet L, Weis J-J (1972) Phys Rev A 5:939
44. Imperio A, Reatto L (2004) Phys J: Condens Matter 16:S3769
45. Peyre V, Spalla O, Belloni L, Nabavi M (1997) Colloid J Interface Sci 187:184
46. Sear RP, Gelbart WM (1999) Chem J Phys 110:4582
47. Sciortino F, Mossa S, Zaccarelli E, Tartaglia P (2004) Phys Rev Lett 93:055701
48. Mossa S, Sciortino F, Tartaglia P, Zaccarelli E (2004) Langmuir 20:10756
49. Liu Y, Chen W-R, Chen S-H (2005) Chem Phys J 122:044507
50. Stradner A, Sedgwick H, Cardinaux F, Poon WCK, Egelhaaf SU, Schurtenberger P (2004) Nature 432:492
51. Hansen JP, Verlet L (1969) Phys Rev 184:151
52. Lang A, Likos CN, Watzlawek M, Löwen H (2000) Phys J: Condens Matter 12:087
53. Likos CN, Lang A, Watzlawek M, Löwen H (2001) Phys Rev E 63:31206
54. Hornreich RM, Liebmann R, Schuster HG, Selke W (1979) Phys Z B 35:91
55. Gompper G, Schick M (1990) Phys Rev B 41:9148
56. Likos CN, Mecke KR, Wagner H (1995) Chem J Phys 102:9350
57. Archer AJ, Likos CN, Evans R (2002) Phys J: Condens Matter 14:12031
58. Archer AJ, Likos CN, Evans R (2004) Phys J: Condens Matter 16:L297
59. Tejero CF, Daanoun A, Lekkerkerker HNW, Baus M (1995) Phys Rev E 51:558
60. Gottwald D, Kahl G, Likos CN (2005) Chem J Phys 122:204503